

# Synthesis and Structures of Triple-Decker Complexes with a Bridging Tetramethylcyclopentadienyl Ligand

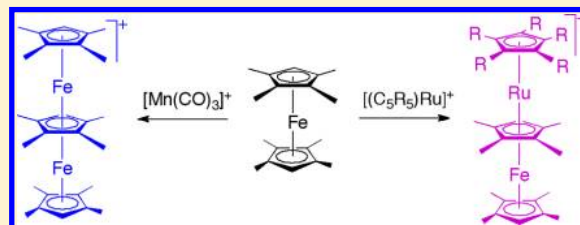
Sonam K. Ghag,<sup>†</sup> Michael L. Tarlton,<sup>†</sup> Ernst A. Henle,<sup>†</sup> Elizabeth M. Ochoa,<sup>†</sup> Alex W. Watson,<sup>†</sup> Lev N. Zakharov,<sup>‡</sup> and Eric J. Watson<sup>\*†</sup>

<sup>†</sup>Department of Chemistry, Seattle University, 901 12th Avenue, Seattle, Washington 98122, United States

<sup>‡</sup>CAMCOR, University of Oregon, 1443 East 13th Avenue, Eugene, Oregon 97403, United States

## Supporting Information

**ABSTRACT:** New triple-decker complexes with bridging tetramethylcyclopentadienyl ligands were synthesized by the reaction of electrophilic metal fragments with octamethylferrocene, Cp'<sub>2</sub>Fe (Cp' = C<sub>5</sub>Me<sub>4</sub>H). The reaction of coordinatively unsaturated ruthenium cations [(C<sub>5</sub>R<sub>5</sub>)Ru]<sup>+</sup> (R = H, CH<sub>3</sub>) with Cp'<sub>2</sub>Fe afforded purple-colored heterometallic triple-decker complexes [(C<sub>5</sub>R<sub>5</sub>)Ru(μ-Cp')-FeCp']<sup>+</sup> by direct electrophilic addition. Surprisingly, the analogous reaction with the coordinatively unsaturated manganese cation [Mn(CO)<sub>3</sub>]<sup>+</sup> and Cp'<sub>2</sub>Fe produced a blue homometallic triple-decker complex, [Cp'Fe(μ-Cp')FeCp']<sup>+</sup>, by ring abstraction and subsequent addition of the newly generated cation [Cp'Fe]<sup>+</sup> to an equivalent of Cp'<sub>2</sub>Fe. Three air-stable triple-decker complexes, [Cp'Fe(μ-Cp')FeCp']<sup>+</sup> (2), [CpRu(μ-Cp')FeCp']<sup>+</sup> (3), and [Cp\*Ru(μ-Cp')FeCp']<sup>+</sup> (4), have been characterized by NMR spectroscopy, elemental analysis, and single-crystal X-ray diffraction.



## INTRODUCTION

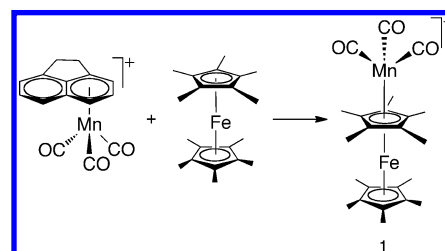
Multimetallic complexes possessing  $\pi$ -conjugated ligands inspire ongoing interest due to their distinctive structural features and the promise of useful applications in the field of molecular electronics.<sup>1–5</sup> In particular, bimetallic multilayer complexes incorporating metallocenes (C<sub>5</sub>R<sub>5</sub>)<sub>2</sub>M attract attention as model systems for the emerging field of bimetallic organometallic sandwich molecular wires (BOSMW).<sup>6–11</sup> Within a BOSMW, electronic communication between the two metal centers may be mediated by a bridging C<sub>5</sub>  $\pi$ -ligand.<sup>12–14</sup> Yet since the discovery of the first triple-decker complex [Ni<sub>2</sub>(C<sub>5</sub>H<sub>5</sub>)<sub>3</sub>]<sup>+</sup> in 1972, other transition metal complexes with C<sub>5</sub>  $\pi$ -ligands remain relatively rare.<sup>15,16</sup>

Furthermore among these complexes, only cyclopentadienyl (Cp = C<sub>5</sub>H<sub>5</sub>) and pentamethylcyclopentadienyl (Cp\* = C<sub>5</sub>Me<sub>5</sub>) rings have been incorporated as bridging ligands.<sup>17–20</sup>

As a unique example of the latter, Sweigart et al. prepared unsymmetrical triple-layer complexes of the iron group by the electrophilic addition of the [Mn(CO)<sub>3</sub>]<sup>+</sup> moiety to a Cp\* ring of decamethylmetallocenes of Fe, Ru, and Os.<sup>21</sup> As shown in Scheme 1, the electron-rich Cp\*<sub>2</sub>Fe displaced the labile acenaphthene ligand from [( $\eta^6$ -acenaphthene)Mn(CO)<sub>3</sub>]BF<sub>4</sub>, affording the triple-layer complex [Cp\*Fe(μ-Cp\*)Mn(CO)<sub>3</sub>]-BF<sub>4</sub> (1·BF<sub>4</sub>).<sup>22,23</sup>

The chemistry shown in Scheme 1 is an example of an “electrophilic stacking reaction” in which a coordinatively unsaturated metal complex fragment adds to a nucleophilic sandwich complex, producing a cationic triple-decker complex.<sup>24,25</sup> In 1976, Hoffmann et al. predicted the stability of triple-decker complexes possessing 30 or 34 valence electrons, and thus the stability of monocation 1 may be understood in

**Scheme 1. Synthesis of Cationic Triple-Decker 1 by Stacking of Decamethylferrocene with a Manganese Tricarbonyl Fragment**



terms of the combination of a 12 valence electron (VE) manganese complex fragment with an 18 VE metallocene to produce a 30 VE triple-layer complex.<sup>26</sup>

## RESULTS AND DISCUSSION

Although initial attempts to grow crystals of [Cp\*Fe(μ-Cp\*)Mn(CO)<sub>3</sub>]BF<sub>4</sub> were not successful, recent experiments afforded green crystals of 1·PF<sub>6</sub> suitable for X-ray analysis.<sup>21</sup> As shown in Figure 1, the structure of 1 confirms the coordination of the [Mn(CO)<sub>3</sub>]<sup>+</sup> fragment to a Cp\* ring of decamethylferrocene and reveals that the manganese tricarbonyl stacked metallocene contains two perfectly staggered Cp\* rings. Similarly, the two Cp\* rings in free decamethylferrocene adopt a staggered conformation in the solid state.<sup>27</sup>

**Received:** December 27, 2012

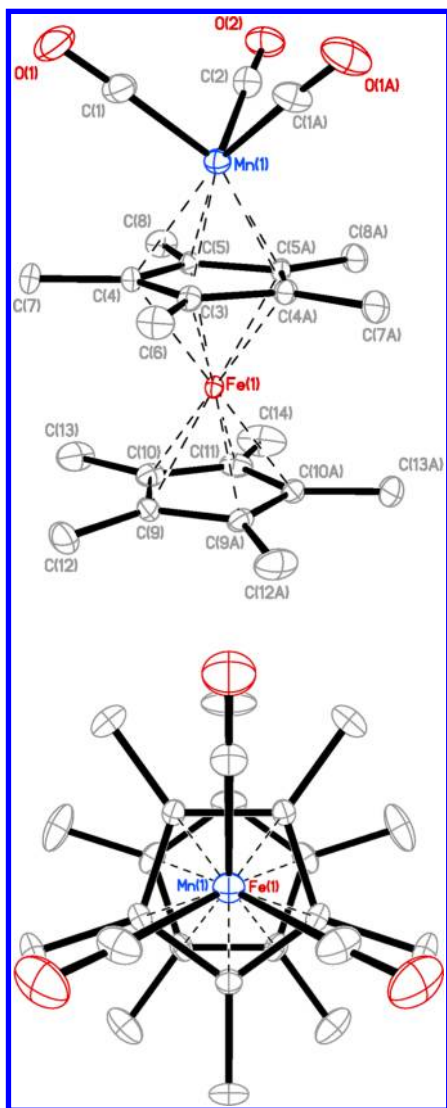
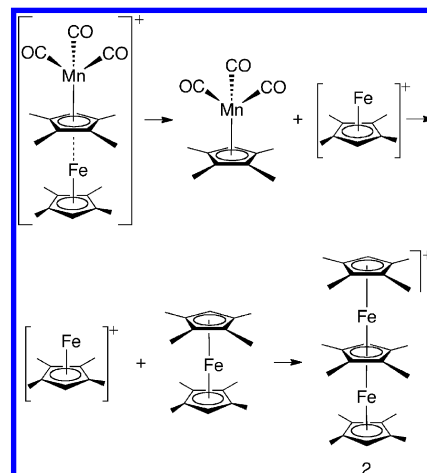


**Figure 1.** ORTEP view of the cation **1** with thermal ellipsoids drawn at the 30% probability level. Selected bond lengths and angles: Mn–C(3) 2.195(4) Å, Mn–C(4) 2.180(3) Å, Mn–C(5) 2.163(3) Å, Fe–C(3) 2.081(4) Å, Fe–C(4) 2.076(3) Å, Fe–C(5) 2.069(3) Å; O(1)–C(1)–Mn 176.8(4)°, O(2)–C(2)–Mn 175.4(5)°. Hydrogen atoms are omitted for clarity.

In light of the chemistry shown in Scheme 1, it was anticipated that the reaction of the same electrophilic reagent  $[(\eta^6\text{-acenaphthene})\text{Mn}(\text{CO})_3]\text{BF}_4$  with octamethylferrocene might yield  $[\text{Cp}'\text{Fe}(\mu\text{-Cp}')\text{Mn}(\text{CO})_3]\text{BF}_4$  by transfer of the  $[\text{Mn}(\text{CO})_3]^+$  moiety to one of the  $\text{Cp}'$  rings of  $\text{Cp}'_2\text{Fe}$ . Instead, the reaction produced a homometallic triple-decker complex,  $[\text{Cp}'\text{Fe}(\mu\text{-Cp}')\text{FeCp}']\text{BF}_4 \cdot 2\text{BF}_4$ , and none of the expected Fe–Mn product. Although  $[\text{Cp}'\text{Fe}(\mu\text{-Cp}')\text{Mn}(\text{CO})_3]\text{BF}_4$  was not observed, it remains a plausible intermediate in the formation of  $2\cdot\text{BF}_4$  since its degradation liberates neutral  $\eta^5\text{-Cp}'\text{Mn}(\text{CO})_3$  (observed by IR analysis,  $\nu_{\text{CO}} = 2006, 1918 \text{ cm}^{-1}$ ) and by mass and charge balance the 12 VE monocation  $[\eta^5\text{-Cp}'\text{Fe}]^+$ . As shown in Scheme 2, this newly generated iron species then combines with an equivalent of  $\text{Cp}'_2\text{Fe}$  to afford the 30 VE cationic triple-decker complex,  $2\cdot\text{BF}_4$ .

In support of this mechanism, Chung and co-workers demonstrated the involvement of triple-layer manganese tricarbonyl cations in ring abstraction reactions.<sup>28,29</sup> Addition-

## Scheme 2. Proposed Mechanism for the Reaction of Manganese Tricarbonyl Cation with Octamethylferrocene



ally, Herberich and co-workers reported a ring ligand transfer reaction in the mechanism for the formation of a diruthenium triple-decker complex,  $[\text{Cp}^*\text{Ru}(\mu\text{-Cp})\text{RuCp}^*]^+$ .<sup>19,30</sup> In related chemistry, the formation of  $[\text{CpNi}(\mu\text{-Cp})\text{NiCp}]^+$  occurred through the reaction of nickelocene with electrophilic species such as  $\text{HBF}_4$ ,  $\text{Ph}_3\text{CBF}_4$ , or  $\text{C}_7\text{H}_7\text{BF}_4$ .<sup>31,32</sup> However the reaction of  $\text{Cp}'_2\text{Fe}$  with  $\text{Ph}_3\text{CBF}_4$  yielded only the oxidation product,  $[\text{Cp}'_2\text{Fe}]\text{BF}_4$ , suggesting the necessity of electrophilic  $\pi$ -complexation for triple-decker formation from highly stable metallocenes. It is noteworthy that Schemes 1 and 2 reveal a remarkable change in reactivity arising from a relatively minor difference in the degree of alkylation in the metallocene, namely, decamethylferrocene or octamethylferrocene.

Blue crystals of  $2\cdot\text{BF}_4$  were obtained and X-ray diffraction analysis confirmed its identity as a homometallic triple-decker complex containing three parallel  $\text{Cp}'$  ligands and two intercalated iron atoms (Figure 2).

The three  $\text{Cp}'$  rings in **2** are almost coplanar: the dihedral tilt angle between the plane of the bridging ring (C1–C5) and terminal ring (C10–C14) is  $2.86(2)^\circ$ , while for the bridge and

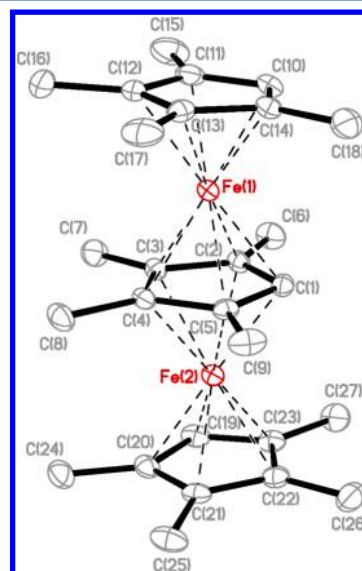


**Figure 2.** ORTEP view of the cation **2** with thermal ellipsoids at the 30% level. Hydrogen atoms are omitted for clarity.

terminal ring (C19–C23) the angle is  $1.69(1)^\circ$ . In addition, the three Cp' decks are highly planar with rms (root-mean-square) deviations of  $0.0007 \text{ \AA}$  (C1–C5),  $0.0030 \text{ \AA}$  (C10–C14), and  $0.0003 \text{ \AA}$  (C19–C23). The methyl groups on the outer Cp' rings incline away from the Fe atoms by  $0.012(5)$  to  $0.079(4) \text{ \AA}$ , while the methyl groups on the inner ring deviate from the plane by only  $0.003(4)$  to  $0.024(4) \text{ \AA}$ . The intramolecular Fe...Fe distance,  $3.3153(5) \text{ \AA}$ , is considerably longer than the sum of the covalent radii (estimated at  $2.6$  to  $3.0 \text{ \AA}$ ), and therefore any direct Fe...Fe interaction is unlikely.<sup>33,34</sup> Instead, electronic communication between the iron atoms may be mediated by the bridging  $\pi$ -ligand.<sup>2,35,36</sup>

Table 1 shows that for the two terminal Cp' ligands in **2**, Fe–C bond distances are close to the corresponding distances

**Table 1.** Selected Bond Lengths (*d*) in the Complex **2**·BF<sub>4</sub>

M–bridging ligand		M–terminal ligand	
bond	<i>d</i> /Å	bond	<i>d</i> /Å
Fe(1)–C(1)	2.054(2)	Fe(1)–C(10)	2.026(2)
Fe(1)–C(2)	2.072(2)	Fe(1)–C(11)	2.064(2)
Fe(1)–C(3)	2.084(2)	Fe(1)–C(12)	2.061(2)
Fe(1)–C(4)	2.078(2)	Fe(1)–C(13)	2.056(2)
Fe(1)–C(5)	2.065(2)	Fe(1)–C(14)	2.043(2)
Fe(1)···Cp'	1.657(1)	Fe(1)···Cp'	1.653(1)
Fe(2)–C(1)	2.055(2)	Fe(2)–C(19)	2.039(2)
Fe(2)–C(2)	2.072(2)	Fe(2)–C(20)	2.059(2)
Fe(2)–C(3)	2.084(2)	Fe(2)–C(21)	2.053(2)
Fe(2)–C(4)	2.077(2)	Fe(2)–C(22)	2.049(2)
Fe(2)–C(5)	2.069(2)	Fe(2)–C(23)	2.049(2)
Fe(2)···Cp'	1.658(1)	Fe(2)···Cp'	1.652(1)

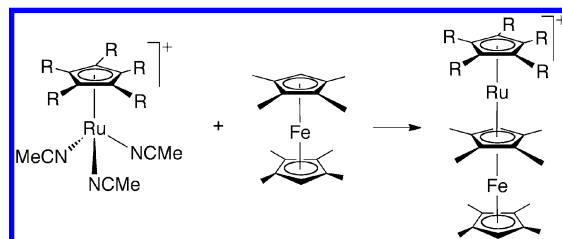
in free octamethylferrocene (Fe–C  $2.048 \text{ \AA}$ , C–C  $1.422 \text{ \AA}$ ),<sup>37,38</sup> but for the bridging ligand, the average Fe–C bond is longer ( $2.071 \text{ \AA}$ ), as are the C–C bonds within the Cp' ring (average  $1.460 \text{ \AA}$ ). Moreover, the average perpendicular distance between each Fe and the center of the bridging Cp' ring is slightly longer ( $1.658 \text{ \AA}$ ) than the corresponding distance to the center of the outer rings ( $1.652 \text{ \AA}$ ). Insofar as bond length can be correlated with bond strength, these data suggest weaker Fe–C and C–C interactions for the bifacially coordinated bridging ring compared with the singly coordinated terminal rings.<sup>39,40</sup> Table 1 also shows that the unsubstituted carbons within each tetramethylcyclopentadienyl ring (C1, C10, and C19) of **2** are significantly closer to the iron atom (ca.  $0.02 \text{ \AA}$ ) than are the methylated carbons. This same asymmetry is evident in the parent metallocene Cp'₂Fe and its monocation [Cp'₂Fe]BF₄, both of which display shorter Fe–C bonds to the one unsubstituted carbon within each Cp' ligand.<sup>37,41</sup>

The two terminal rings in **2** are nearly eclipsed with torsion angles for C(10–14)–Ct'–Ct''–C(19–23) between  $3.8^\circ$  and  $4.4^\circ$  (Ct = ring centroid), whereas the bridging ring is rotated by approximately  $33^\circ$  for C(1–5)–Ct–Ct'–C(10–14) and  $29^\circ$  for C(1–5)–Ct–Ct''–C(19–23).<sup>20</sup> These cross-orientation angles differ from the solid-state structure of octamethylferrocene, in which the two Cp' rings are staggered perfectly and the unsubstituted carbon on each Cp' ring is rotated by  $180^\circ$  from the other.<sup>37,38,41</sup>

In contrast with the manganese chemistry, reaction of ruthenium cations [CpRu(NCMe)₃]⁺ and [Cp\*Ru(NCMe)₃]⁺ with Cp'₂Fe did not bring about ring abstraction. Rather each ruthenium complex eliminated acetonitrile to generate a 12 VE

metal complex fragment, which then coordinated to a Cp' ligand of the sandwich compound, producing a stable 30 VE heterometallic triple-decker complex (Scheme 3).

**Scheme 3.** Synthesis of [Cp(R)Ru(μ-Cp')FeCp']⁺, **3** (R = H) and **4** (R = Me)



Thus an electrophilic stacking reaction of [CpRu]PF₆ with Cp'₂Fe afforded purple **3**·PF₆ in moderate yield, and reaction of [Cp\*Ru]PF₆ with Cp'₂Fe produced light purple **4**·PF₆ in excellent yield. The structure of cation **3** was determined by single-crystal X-ray diffraction and confirmed that the ruthenium and iron atoms are located between three parallel cyclopentadienyl systems. (Figure 3).

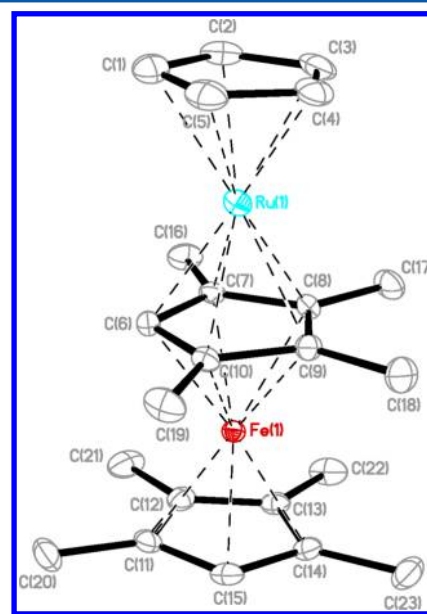


**Figure 3.** ORTEP view of **3** with displacement ellipsoids at the 30% level. Hydrogen atoms are omitted for clarity.

In **3**, the dihedral tilt angle between Cp(C1–C5) and Cp'(C6–C10) is  $2.11(3)^\circ$ , and between Cp'(C6–C10) and Cp'(C11–C15) the angle is  $2.45(3)^\circ$ . The Cp ring is highly planar (rms deviation of  $0.0028 \text{ \AA}$ ), as are the two Cp' rings (rms deviations of  $0.0010$  and  $0.0012 \text{ \AA}$ ). The four methyl groups deviate from the plane of the middle deck by  $0.0012(8)$  to  $0.020(8) \text{ \AA}$ , while those on the outer Cp' ring incline away from the iron atom by  $0.021(8)$  to  $0.071(8) \text{ \AA}$ . The intramolecular Fe...Ru distance is  $3.4700(6) \text{ \AA}$ , which exceeds the sum of Ru...Fe covalent radii ( $2.98 \text{ \AA}$ ), indicating the absence of a direct metal–metal bond.<sup>1,4,34</sup>

As shown in Table 2, the average distance between the Fe atom and its terminal ring carbons is  $2.057 \text{ \AA}$ , while the distance to the bridging ring carbons is  $2.077 \text{ \AA}$ . Similarly, the average Ru–C(Cp) distance is  $2.160 \text{ \AA}$ , while the Ru–C(Cp')

Table 2. Selected Bond Lengths (*d*) in the Complex 3·PF<sub>6</sub>

M–bridging ligand		M–terminal ligands	
bond	<i>d</i> /Å	bond	<i>d</i> /Å
Ru(1)–C(6)	2.187(4)	Ru(1)–C(1)	2.180(5)
Ru(1)–C(7)	2.186(4)	Ru(1)–C(2)	2.160(5)
Ru(1)–C(8)	2.193(4)	Ru(1)–C(3)	2.151(4)
Ru(1)–C(9)	2.204(4)	Ru(1)–C(4)	2.153(4)
Ru(1)–C(10)	2.215(4)	Ru(1)–C(5)	2.155(5)
Ru(1)⋯Cp'	1.809(2)	Ru(1)⋯Cp	1.792(2)
Fe(1)–C(6)	2.057(4)	Fe(1)–C(11)	2.054(4)
Fe(1)–C(7)	2.078(4)	Fe(1)–C(12)	2.062(4)
Fe(1)–C(8)	2.091(4)	Fe(1)–C(13)	2.065(4)
Fe(1)–C(9)	2.086(4)	Fe(1)–C(14)	2.057(4)
Fe(1)–C(10)	2.075(4)	Fe(1)–C(15)	2.045(4)
Fe(1)⋯Cp'	1.661(2)	Fe(1)⋯Cp'	1.660(2)

distance is almost 0.04 Å longer (average 2.197 Å). The average C–C bond in the central ring is 1.467 Å but only 1.428 Å for the outer Cp'. Therefore as with bimetallic complex 2, formation of 3 from Cp'<sub>2</sub>Fe elongated the Fe–C and C–C bonds for the bridging Cp' ligand relative to the terminal Cp' ligand.

In 3 none of the rings is staggered as in free octamethylferrocene, but instead the cross-orientation for the two Cp' rings, C(6–10)–Ct'–Ct''(C11–C15), ranges from 19.0° to 19.7° (average 19.3°). The Cp ring and bridging Cp' ring are almost eclipsed, with torsion angles of only 1.9° to 4.0° (average 3.1°) for C(1–5)–Ct–Ct'–C(6–10), while the Cp ring and the terminal Cp'(C11–C15) are rotated by an average of 22.4°.

For Ru–Fe complex 4, X-ray diffraction analysis revealed two symmetrically independent triple-decker complexes in the unit cell (Figure 4). The three parallel carbocyclic ligands are nearly coplanar in both conformations: in 4A, the dihedral tilt angle between Cp\*(C1–C5) and Cp'(C6–C10) is 0.60(5)° and between Cp'(C6–C10) and Cp'(C11–C15) the angle is 2.85(5)°; in 4B, the dihedral tilt angle between Cp\*(C1–C5) and Cp'(C6'–C10') is 1.85(5)° and between Cp'(C6'–C10') and Cp'(C11'–C15') the angle is 3.44(5)°. The intramolecular distances between the iron and ruthenium atoms are similar in both conformations: 3.4703(9) Å for 4A and 3.4762(9) Å for 4B. In both rotamers of 4, the methyl groups of the terminal Cp' rings incline away from the Fe atom by 0.004(1) to 0.090(1) Å, and the five methyl groups on the Cp\* ring bend away from the Ru atom by 0.005(1) to 0.053(1) Å. The methyl groups of the bridging Cp' rings are more planar, deviating from the plane of the central ring by 0.004(1) to 0.039(1) Å.

Comparison of selected bond lengths in 4A and 4B reveals close similarities between the two rotational conformers. As shown in Table 3, the Fe–C bonds to the bridging ring are longer for conformer 4A (average 2.053 Å) than 4B (average 2.046 Å), whereas the Fe–C bonds for the terminal ring are longer for conformer 4B (average 2.064 Å) than 4A (average 2.058 Å). Thus unlike 2 and 3, complex 4 has shorter Fe–C bonds for the bridging ligand than for the terminal ligand. Moreover, the perpendicular distance from the iron atom to the center of the bridging ring is shorter than the distance to the outer ring for both conformations. The average C–C bonds in the three rings do not differ significantly between 4A and 4B: the average C–C bonds in 4A are 1.423 Å (Cp\*), 1.421 Å (Cp', terminal), and 1.451 Å (Cp', bridge); the average C–C

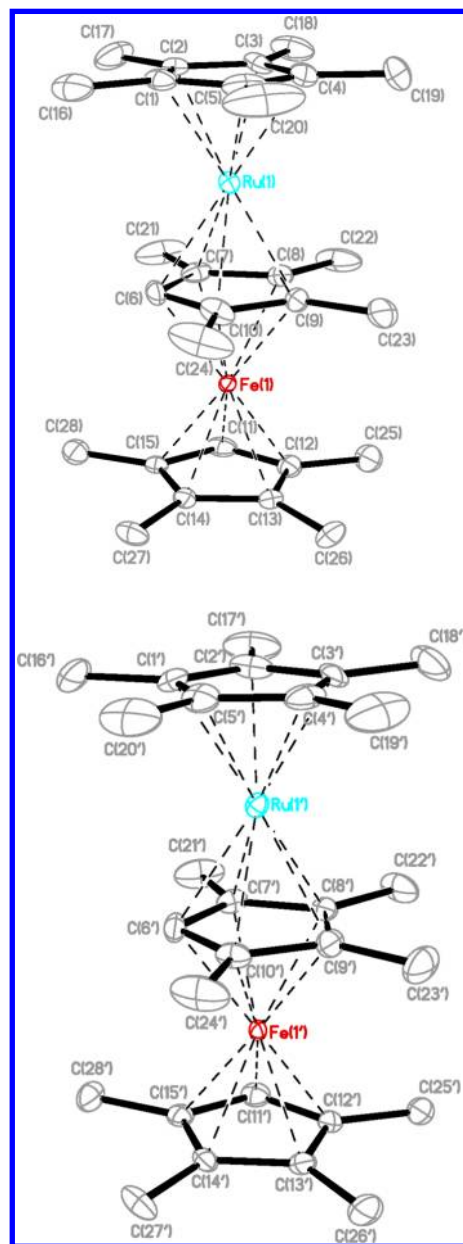


Figure 4. ORTEP views of complexes 4A (top) and 4B (bottom) with displacement ellipsoids at the 30% level. Hydrogen atoms are omitted for clarity.

bonds in 4B are 1.416 Å (Cp\*), 1.424 Å (Cp', terminal), and 1.448 Å (Cp', bridge).

While the two rotational conformers are neither fully eclipsed nor staggered, Figure 5 shows that the cross orientation of the two Cp' rings and Cp\* ring is closer to an eclipsed conformation in 4B than in 4A. In the rotational conformer 4A, the average torsion angle between Cp\* and the bridging Cp' is 20.7°, while the two Cp' rings are rotated by 23.9°. For 4B, the average torsion angle between the Cp\* ring and the bridging Cp' is 18.9°, while the two Cp' rings are rotated by 19.9°. Therefore for 4B, the two terminal rings are nearly eclipsed (average torsion angle 1.0°) compared with a more staggered geometry of 44.5° for the terminal rings in 4A.

Table 4 presents results from <sup>1</sup>H NMR, <sup>13</sup>C NMR, and 2-D HMQC experiments for the three 30 VE monocations 2–4. <sup>1</sup>H NMR data reveal that the signals for protons on the terminal

Table 3. Selected Bond Lengths (*d*) in 4A·PF<sub>6</sub><sup>-</sup> and 4B·PF<sub>6</sub><sup>-</sup><sup>a</sup>

M-bridging ligand		M-terminal ligands	
bond	<i>d</i> /Å	bond	<i>d</i> /Å
Ru(1)–C(6)	2.195(6)	Ru(1)–C(1)	2.161(6)
Ru(1)–C(7)	2.204(5)	Ru(1)–C(2)	2.161(6)
Ru(1)–C(8)	2.203(5)	Ru(1)–C(3)	2.168(6)
Ru(1)–C(9)	2.217(6)	Ru(1)–C(4)	2.148(6)
Ru(1)–C(10)	2.216(6)	Ru(1)–C(5)	2.145(6)
Ru(1)⋯Cp'	1.829(3)	Ru(1)⋯Cp*	1.785(3)
Fe(1)–C(6)	2.034(6)	Fe(1)–C(11)	2.051(6)
Fe(1)–C(7)	2.049(6)	Fe(1)–C(12)	2.058(6)
Fe(1)–C(8)	2.070(6)	Fe(1)–C(13)	2.068(5)
Fe(1)–C(9)	2.065(6)	Fe(1)–C(14)	2.056(5)
Fe(1)–C(10)	2.049(6)	Fe(1)–C(15)	2.057(5)
Fe(1)⋯Cp'	1.641(3)	Fe(1)⋯Cp'	1.666(3)
Ru(1')–C(6')	2.200(6)	Ru(1')–C(1')	2.143(6)
Ru(1')–C(7')	2.210(5)	Ru(1')–C(2')	2.147(6)
Ru(1')–C(8')	2.215(5)	Ru(1')–C(3')	2.146(6)
Ru(1')–C(9')	2.235(6)	Ru(1')–C(4')	2.138(6)
Ru(1')–C(10')	2.032(6)	Ru(1')–C(5')	2.143(6)
Ru(1')⋯Cp'	1.843(3)	Ru(1')⋯Cp*	1.773(3)
Fe(1')–C(6')	2.029(6)	Fe(1')–C(11')	2.066(6)
Fe(1')–C(7')	2.044(5)	Fe(1')–C(12')	2.074(6)
Fe(1')–C(8')	2.069(5)	Fe(1')–C(13')	2.072(5)
Fe(1')–C(9')	2.054(6)	Fe(1')–C(14')	2.065(5)
Fe(1')–C(10')	2.032(6)	Fe(1')–C(15')	2.045(5)
Fe(1')⋯Cp'	1.633(3)	Fe(1')⋯Cp'	1.671(3)

<sup>a</sup>Atom labels for complex 4B are designated with primes.

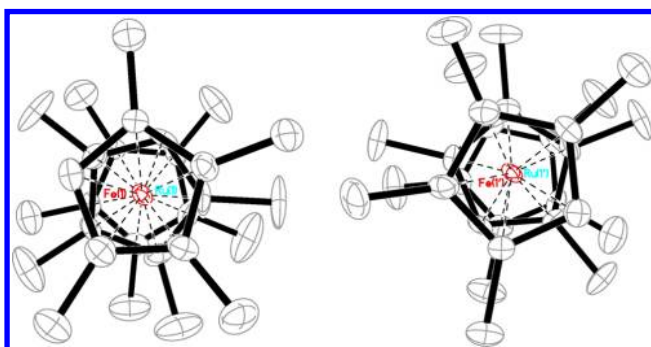


Figure 5. ORTEP views of complexes 4A (left) and 4B (right) along the Fe⋯Ru line with displacement ellipsoids at the 30% level. Hydrogen atoms are omitted for clarity.

Cp' rings in the triple-decker complexes are close to those of free octamethylferrocene:  $\delta$  3.33 (s, 2H) for hydrogens on the

Table 4. <sup>1</sup>H and <sup>13</sup>C NMR Data for 2–4 and Octamethylferrocene in CD<sub>2</sub>Cl<sub>2</sub>

complex		<sup>1</sup> H NMR, $\delta$ (ppm)			<sup>13</sup> C NMR, $\delta$ (ppm)		
		$\eta^5$ -Cp(R)	$\mu$ - $\eta^5$ : $\eta^5$ -Cp'	$\eta^5$ -Cp'	$\eta^5$ -Cp(R)	$\mu$ - $\eta^5$ : $\eta^5$ -Cp'	$\eta^5$ -Cp'
2 <sup>a</sup>	methyl	1.59, 1.69	2.53, 2.54	1.59, 1.69	8.5, 10.4	11.5, 13.1	8.5, 10.4
	ring	3.45	3.99	3.45	69.4, 80.8, 81.6	58.7, 67.6, 69.0	69.4, 80.8, 81.6
3 <sup>b</sup>	methyl		2.57, 2.69	1.68, 1.79		13.8, 15.2	8.6, 10.4
	ring	4.37	4.65	3.63	73.3	59.5, 69.4, 71.0	73.7, 81.0, 81.7
4 <sup>c</sup>	methyl	1.53	2.31, 2.33	1.70, 1.79	9.6	11.3, 12.9	8.8, 10.6
	ring		4.05	3.62	85.3	60.2, 69.1, 69.8	71.0, 81.2, 81.9
Cp' <sub>2</sub> Fe	methyl			1.69, 1.73			9.8, 11.8
	ring			3.33			71.0, 80.3, 80.5

<sup>a</sup>Cp(R) = C<sub>3</sub>Me<sub>4</sub>H. <sup>b</sup>Cp(R) = C<sub>3</sub>H<sub>5</sub>. <sup>c</sup>Cp(R) = C<sub>3</sub>Me<sub>5</sub>.

ring and  $\delta$  1.69 (s, 12H) and 1.73 (s, 12H) for hydrogens on the methyl group. In contrast, signals for the 12 methyl protons and one ring proton on the bridging Cp' are shifted downfield of these values by 0.6 to 1.3 ppm. Similarly <sup>13</sup>C resonances for the terminal ligands of the triple-deckers are near those for free Cp'<sub>2</sub>Fe ( $\delta$  71.0 (2C), 80.3 (4C), 80.5 (4C) and  $\delta$  9.8 (4C), 11.8 (4C)). However, for the bridging position, signals for methyl carbons are shifted downfield of these by 1.1 to 4.0 ppm, and ring carbons are shifted upfield by 9.5 to 12.7 ppm. HMQC experiments confirmed the assignment of the signals for the Cp' methyl carbons in 3 and 4, whereas in 2 their assignment was unambiguous since [Cp'Fe( $\mu$ -Cp')FeCp']<sup>+</sup> possesses two identical terminal Cp' rings. Within each tetramethylcyclopentadienyl ring, the <sup>13</sup>C resonance of the unsubstituted carbon is upfield of the resonance for the methylated ring carbons by 7.4 to 12.2 ppm. These spectroscopic data correlate with structural information (Tables 1, 2, and 3) that shows that in the solid state the unsubstituted carbon on each Cp' ring is typically closer to the iron atom than are the methylated ring carbons.

The NMR spectroscopy of 2–4 shares key features with the other bimetallic triple-decker complexes. In their pioneering research with iron group complexes, Rybinskaya and Kudinov and co-workers reported a downfield shift for protons on Cp\* ligands in the bridging position and an upfield shift of their ring carbons (Table 5).<sup>17–19</sup> Similarly for complexes 2–4, bifacial

Table 5. <sup>1</sup>H and <sup>13</sup>C NMR Data for [CpFe( $\mu$ -Cp)FeCp]PF<sub>6</sub>,<sup>18</sup> [CpFe( $\mu$ -Cp\*)FeCp\*]PF<sub>6</sub>,<sup>17</sup> [CpFe( $\mu$ -Cp\*)RuCp\*]PF<sub>6</sub>,<sup>17</sup> and [Cp\*Ru( $\mu$ -Cp\*)FeCp\*]PF<sub>6</sub><sup>42</sup> in CD<sub>2</sub>Cl<sub>2</sub>

complex	<sup>1</sup> H NMR, $\delta$ (ppm)			<sup>13</sup> C NMR, $\delta$ (ppm)		
	$\eta^5$ -Cp(R) Fe	$\mu$ - $\eta^5$ : $\eta^5$ -Cp(R)	$\eta^5$ -Cp(R)	$\eta^5$ -Cp(R) Fe	$\mu$ - $\eta^5$ : $\eta^5$ -Cp(R)	$\eta^5$ -Cp(R)
CpFe( $\mu$ -Cp)FeCp	4.37	4.37	4.37	69.2	52.5	69.2
CpFe( $\mu$ -Cp*)FeCp*	3.87	2.69	1.51	71.9	8.3, 69.1	13.3, 79.2
CpFe( $\mu$ -Cp*)RuCp*	4.09	2.56	1.43	72.4	9.2, 71.1	13.7, 84.9
Cp*Fe( $\mu$ -Cp*)RuCp*	1.65	2.32	1.44	8.4, 79.4	11.4, 69.9	9.1, 84.6

coordination to the bridging Cp' ring brought about a downfield shift of its proton signals and an upfield shift for its ring carbon signals (Table 4). Thus for this class of compounds, coordination of two transition metals to opposing

faces of a bridging ligand almost always distinguishes its NMR signals from those of the singly coordinated terminal ligands. However this difference is less pronounced in some triple-decker complexes,<sup>43</sup> and indeed for [CpFe( $\mu$ -Cp)FeCp], <sup>1</sup>H NMR spectroscopy revealed a single resonance for all three rings.<sup>18</sup>

## CONCLUSION

In 2001, Sweigart et al. demonstrated that the manganese tricarbonyl transfer reagent [( $\eta^6$ -acenaphthene)Mn(CO)<sub>3</sub>]BF<sub>4</sub> reacted with electron-rich decamethylferrocene to produce the triple-layer complex **1**·BF<sub>4</sub>. Extending this methodology to octamethylferrocene did not afford the analogous Fe–Mn stacking product, but instead produced **2**·BF<sub>4</sub>, a novel diiron triple-decker by a more complicated mechanism involving ring abstraction and subsequent electrophilic addition. Comparison of the chemistry of complexes **1** and **2** points to a dramatic change in reactivity based on a relatively subtle difference in the degree of alkylation of the bridging ligand, namely, C<sub>5</sub>Me<sub>5</sub> vs C<sub>5</sub>Me<sub>4</sub>H. In contrast with the manganese chemistry, two ruthenium cations, [CpRu]<sup>+</sup> and [Cp\*Ru]<sup>+</sup>, produced stable coordination products with octamethylferrocene by an electrophilic stacking mechanism and yielded two heterometallic triple-decker complexes, **3**·PF<sub>6</sub> and **4**·PF<sub>6</sub>.

## EXPERIMENTAL SECTION

**General Experimental Methods.** All reactions were carried out under an atmosphere of dry nitrogen. Dichloromethane was collected from a Braun MBS-800 solvent purification system immediately before use. All other solvents were purchased from commercial sources and used without further purification. [CpRu(NCMe)<sub>3</sub>]PF<sub>6</sub>,<sup>44</sup> [Cp\*Ru(NCMe)<sub>3</sub>]PF<sub>6</sub>,<sup>45</sup> and octamethylferrocene or bis(tetramethyl)cyclopentadienyl iron(II) were synthesized according to literature methods or purchased from Strem Chemicals Inc. [( $\eta^6$ -Acenaphthene)Mn(CO)<sub>3</sub>]BF<sub>4</sub> was prepared according to literature methods.<sup>46</sup> <sup>1</sup>H and <sup>13</sup>C{<sup>1</sup>H} NMR spectra were recorded at 400.1 and 100.6 MHz, respectively, and at ambient temperatures. All chemical shifts are reported in  $\delta$  units referenced to the internal standards for the deuterated solvents. Elemental analyses were carried out by Atlantic Microlab Inc.

[(C<sub>5</sub>(CH<sub>3</sub>)<sub>4</sub>H)Fe( $\mu$ -C<sub>5</sub>(CH<sub>3</sub>)<sub>4</sub>H)Fe(C<sub>5</sub>(CH<sub>3</sub>)<sub>4</sub>H)]BF<sub>4</sub> (**2**·BF<sub>4</sub>). [( $\eta^6$ -acenaphthene)Mn(CO)<sub>3</sub>]BF<sub>4</sub> (0.200 g, 0.526 mmol), Cp'Fe (0.330 g, 1.105 mmol), and 40 mL of CH<sub>2</sub>Cl<sub>2</sub> were mixed under N<sub>2</sub> and heated to reflux for 2 h. During the course of the reaction, the solution color changed from orange to blue. The reaction may be monitored for completion by IR since the neutral side product  $\eta^5$ -Cp'Mn(CO)<sub>3</sub> has bands at  $\nu_{\text{CO}}$  = 2006 (s), 1918 (s, br) cm<sup>-1</sup> distinct from the starting cation [( $\eta^6$ -acenaphthene)Mn(CO)<sub>3</sub>]BF<sub>4</sub> at  $\nu_{\text{CO}}$  = 2072 (s), 2012 (s, br) cm<sup>-1</sup>. The solution was cooled to room temperature and concentrated to about 2 mL under N<sub>2</sub> flow. Addition of 70 mL of diethyl ether precipitated a blue powder. The solid was washed with diethyl ether (2 × 10 mL) and then placed on a short silica gel column prepared with CH<sub>2</sub>Cl<sub>2</sub>. The deep blue product eluted with a 1:5 mixture of CH<sub>3</sub>NO<sub>2</sub>/CH<sub>2</sub>Cl<sub>2</sub>, and the solvent was removed *in vacuo* to yield **2**·BF<sub>4</sub> as a blue solid. In some instances, a small amount of green [Cp'Fe]BF<sub>4</sub> eluted with the product. This could be separated cleanly from **2**·BF<sub>4</sub> on a silica gel TLC plate with a 1:10 mixture of acetone/CH<sub>2</sub>Cl<sub>2</sub>. Yield: 0.136 g (46%). <sup>1</sup>H NMR (CD<sub>2</sub>Cl<sub>2</sub>):  $\delta$  3.99 (s, 1H,  $\mu$ -C<sub>5</sub>(CH<sub>3</sub>)<sub>4</sub>H), 3.45 (s, 2H, C<sub>5</sub>(CH<sub>3</sub>)<sub>4</sub>H), 2.53 (s, 6H,  $\mu$ -C<sub>5</sub>(CH<sub>3</sub>)<sub>4</sub>H), 2.54 (s, 6H,  $\mu$ -C<sub>5</sub>(CH<sub>3</sub>)<sub>4</sub>H), 1.69 (s, 12H, C<sub>5</sub>(CH<sub>3</sub>)<sub>4</sub>H), 1.59 (s, 12H, C<sub>5</sub>(CH<sub>3</sub>)<sub>4</sub>H). <sup>13</sup>C{<sup>1</sup>H} NMR (CD<sub>2</sub>Cl<sub>2</sub>):  $\delta$  81.6, 80.8, 69.4, 69.0, 67.6, 58.7, 13.1, 11.5, 10.4, 8.5. Anal. Calcd for C<sub>27</sub>H<sub>39</sub>Fe<sub>2</sub>BF<sub>4</sub>: C, 57.65; H, 6.99. Found: C, 57.60; H, 7.02.

[(C<sub>5</sub>H<sub>5</sub>)Ru( $\mu$ -C<sub>5</sub>(CH<sub>3</sub>)<sub>4</sub>H)Fe(C<sub>5</sub>(CH<sub>3</sub>)<sub>4</sub>H)]PF<sub>6</sub> (**3**·PF<sub>6</sub>). [CpRu(NCMe)<sub>3</sub>]PF<sub>6</sub> (0.150 g, 0.345 mmol), Cp'Fe (0.115 g, 0.386 mmol), and 40 mL of CH<sub>2</sub>Cl<sub>2</sub> were mixed under N<sub>2</sub>. The solution was refluxed for 4 h, during which time the solution changed gradually

from brown to dark purple. After cooling to room temperature, the solution was concentrated under N<sub>2</sub> flow to about 2 mL. Addition of 50 mL of diethyl ether precipitated a purple solid. The solid was washed with diethyl ether (2 × 10 mL) and then placed on a deactivated neutral alumina column (10% H<sub>2</sub>O) prepared with CH<sub>2</sub>Cl<sub>2</sub>. The product was eluted with CH<sub>2</sub>Cl<sub>2</sub>, and the solvent was removed *in vacuo* to yield a purple solid. Yield: 0.088 g (42%). <sup>1</sup>H NMR (CD<sub>2</sub>Cl<sub>2</sub>):  $\delta$  4.65 (s, 1H,  $\mu$ -C<sub>5</sub>(CH<sub>3</sub>)<sub>4</sub>H), 4.37 (s, 5H, C<sub>5</sub>H<sub>5</sub>), 3.63 (s, 1H, C<sub>5</sub>(CH<sub>3</sub>)<sub>4</sub>H), 2.69 (s, 6H,  $\mu$ -C<sub>5</sub>(CH<sub>3</sub>)<sub>4</sub>H), 2.57 (s, 6H,  $\mu$ -C<sub>5</sub>(CH<sub>3</sub>)<sub>4</sub>H), 1.79 (s, 6H, C<sub>5</sub>(CH<sub>3</sub>)<sub>4</sub>H), 1.68 (s, 6H, C<sub>5</sub>(CH<sub>3</sub>)<sub>4</sub>H). <sup>13</sup>C{<sup>1</sup>H} NMR (CD<sub>2</sub>Cl<sub>2</sub>):  $\delta$  81.7, 81.0, 73.7, 73.3, 71.0, 69.4, 59.5, 15.2, 13.8, 10.4, 8.6. Anal. Calcd for C<sub>23</sub>H<sub>31</sub>FeRuPF<sub>6</sub>: C, 45.33; H, 5.13. Found: C, 45.47; H, 5.12.

[(C<sub>5</sub>(CH<sub>3</sub>)<sub>5</sub>)Ru( $\mu$ -C<sub>5</sub>(CH<sub>3</sub>)<sub>4</sub>H)Fe(C<sub>5</sub>(CH<sub>3</sub>)<sub>4</sub>H)]PF<sub>6</sub> (**4**·PF<sub>6</sub>). Cp\*Ru(NCMe)<sub>3</sub>]PF<sub>6</sub> (0.150 g, 0.297 mmol), Cp'Fe (0.098 g, 0.327 mmol), and 40 mL of CH<sub>2</sub>Cl<sub>2</sub> were mixed under N<sub>2</sub>. The solution was refluxed for 2 h, during which time the solution changed quickly from brown to light purple. After cooling to room temperature, the solution was concentrated under N<sub>2</sub> flow to about 2 mL. Addition of 50 mL of diethyl ether precipitated a light purple solid. The solid was washed with diethyl ether (2 × 10 mL) and then placed on a deactivated neutral alumina column (10% H<sub>2</sub>O) prepared with CH<sub>2</sub>Cl<sub>2</sub>. The product was eluted with CH<sub>2</sub>Cl<sub>2</sub>, and the solvent was removed *in vacuo* to yield a light purple solid. Yield: 0.175 g (87%). <sup>1</sup>H NMR (CD<sub>2</sub>Cl<sub>2</sub>):  $\delta$  4.05 (s, 1H,  $\mu$ -C<sub>5</sub>(CH<sub>3</sub>)<sub>4</sub>H), 3.62 (s, 1H, C<sub>5</sub>(CH<sub>3</sub>)<sub>4</sub>H), 2.33 (s, 6H,  $\mu$ -C<sub>5</sub>(CH<sub>3</sub>)<sub>4</sub>H), 2.31 (s, 6H,  $\mu$ -C<sub>5</sub>(CH<sub>3</sub>)<sub>4</sub>H), 1.79 (s, 6H, C<sub>5</sub>(CH<sub>3</sub>)<sub>4</sub>H), 1.70 (s, 6H, C<sub>5</sub>(CH<sub>3</sub>)<sub>4</sub>H), 1.53 (s, 15H, C<sub>5</sub>(CH<sub>3</sub>)<sub>5</sub>). <sup>13</sup>C{<sup>1</sup>H} NMR (CD<sub>2</sub>Cl<sub>2</sub>):  $\delta$  85.3, 81.9, 81.2, 71.0, 69.8, 69.1, 60.2, 12.9, 11.3, 10.6, 9.6, 8.8. Anal. Calcd for C<sub>28</sub>H<sub>41</sub>FeRuPF<sub>6</sub>: C, 49.47; H, 6.08. Found: C, 49.56; H, 6.06.

**X-ray Crystallography.** Crystals for **2**·BF<sub>4</sub>, **3**·PF<sub>6</sub>, and **4**·PF<sub>6</sub> were obtained by the slow vapor diffusion of diethyl ether into CH<sub>2</sub>Cl<sub>2</sub> solutions at -20 °C. Crystals for complex **1**·PF<sub>6</sub> were obtained by the addition of an excess of NH<sub>4</sub>PF<sub>6</sub> prior to vapor diffusion of diethyl ether into a CH<sub>2</sub>Cl<sub>2</sub> solution of **1**·BF<sub>4</sub> at -20 °C. Table 6 (Supporting Information) presents the key crystallographic and structure refinement data. X-ray diffraction experiments were carried out on a Bruker Smart Apex diffractometer at 193 K (**1**·PF<sub>6</sub> and **2**·BF<sub>4</sub>), 173 K (**3**·PF<sub>6</sub>), and 110 K (**4**·PF<sub>6</sub>) using Mo K $\alpha$  radiation ( $\lambda$  = 0.71073 Å). Absorption corrections were applied by SADABS.<sup>47</sup> The structures were solved using direct methods and refined with full-matrix least-squares methods based on F<sup>2</sup>. All non-H atoms were refined with anisotropic thermal parameters. The H atoms in all structures were refined in calculated positions using a rigid group model. The structure of **2**·BF<sub>4</sub> was determined in non-centrosymmetrical space group Cc. The found Flack parameter is 0.500(12), indicating possible space group C2/c. The structure of **2**·BF<sub>4</sub> could be obtained in space group C2/c but with disordered C<sub>5</sub>Me<sub>4</sub>H groups in the Fe<sub>2</sub>(C<sub>5</sub>Me<sub>4</sub>H)<sub>3</sub> cation. The symmetry of the Fe<sub>2</sub>(C<sub>5</sub>Me<sub>4</sub>H)<sub>3</sub> cation is close to but not exactly C<sub>2</sub>. On this basis, it is thought that the correct space group for **2**·BF<sub>4</sub> is Cc, and in this space group there is no disorder for the C<sub>5</sub>Me<sub>4</sub>H groups. The PF<sub>6</sub> anion in **3**·PF<sub>6</sub> is disordered over two positions with the ratio 1:1. The structure of **4**·PF<sub>6</sub> consists of two symmetrically independent units. Attempts to solve the structure in the range of temperatures from 173 K up to ambient temperature failed. At these temperatures, the structure of **4**·PF<sub>6</sub> had triclinic symmetry with disordered molecules; the Fe and Ru atoms shared the same positions, and terminal methyl groups were disordered as well. At 110 K, the structure of **4**·PF<sub>6</sub> was determined to be monoclinic with two symmetrically independent units and without any disorder for the Fe and Ru atoms or the terminal methyl groups. One of three PF<sub>6</sub> anions in **4**·PF<sub>6</sub> is in a general position, and two others are on a 2-fold axis. All calculations were performed using the SHELXTL package.<sup>48</sup>

## ASSOCIATED CONTENT

### Supporting Information

Crystallographic and structure refinement data for complexes **1**–**4**, <sup>1</sup>H, <sup>13</sup>C{<sup>1</sup>H}, and HMQC NMR spectra for complexes **2**–**4**, and X-ray crystallographic data in CIF format for the

structures **1**·PF<sub>6</sub> (CCDC ID: 894675), **2**·BF<sub>4</sub> (CCDC ID: 894674), **3**·PF<sub>6</sub> (CCDC ID: 894673), and **4**·PF<sub>6</sub> (CCDC ID: 894672) are available free of charge via the Internet at <http://pubs.acs.org>.

## AUTHOR INFORMATION

### Corresponding Author

\*E-mail: [watsonel@seattleu.edu](mailto:watsonel@seattleu.edu).

### Notes

The authors declare no competing financial interest.

## ACKNOWLEDGMENTS

This research was supported by an award from Research Corporation for Science Advancement (Award # 20904). We thank the Peach Foundation (S.K.G. and E.M.O), the Murdock College Science Research Program (M.L.T. and E.J.W.), and Seattle University for financial support.

## DEDICATION

This article is dedicated in memoriam to Professor Dwight A. Sweigart.

## REFERENCES

- Ceccon, A.; Santi, S.; Orian, L.; Bisello, A. *Coord. Chem. Rev.* **2004**, *248*, 683.
- Aguirre-Etcheverry, P.; O'Hare, D. *Chem. Rev.* **2010**, *110*, 4839.
- Astruc, D. *Acc. Chem. Res.* **1997**, *30*, 383.
- Santi, S.; Ceccon, A.; Bisello, B.; Durante, C.; Ganis, P.; Orian, L.; Benetollo, F.; Crociani, L. *Organometallics* **2005**, *24*, 4691.
- McCleverty, J. A.; Ward, M. D. *Acc. Chem. Res.* **1998**, *31*, 842.
- Lorenz, V.; Blaurock, S.; Hrib, C. G.; Edelman, F. T. *Organometallics* **2010**, *29*, 4787.
- Da, H.; Jin, H. M.; Lim, K. H.; Yang, S.-W. *J. Phys. Chem. C* **2010**, *114*, 21705.
- Zhang, X.; Tian, Z.; Yang, S.-W.; Wang, J. *J. Phys. Chem. C* **2011**, *115*, 2948.
- Morari, C.; Allmaier, H.; Beiușeanu, F.; Jurcuț, T.; Chioncel, L. *Phys. Rev. B* **2012**, *85*, 085413.
- Bruce, M. I.; Le Guennic, B.; Scoleri, N.; Zaitseva, N. N.; Halet, J.-F. *Organometallics* **2012**, *31*, 4701.
- Parida, P.; Basheer, E. A.; Pati, S. K. *J. Mater. Chem.* **2012**, *22*, 14916.
- Zhou, L.; Yang, S.-W.; Ng, M.-F.; Sullivan, M. B.; Tan, V. B. C.; Shen, L. *J. Am. Chem. Soc.* **2008**, *130*, 4023.
- Hradsky, A.; Bildstein, B.; Schuler, N.; Schottenberger, H.; Jaitner, P.; Ongania, K.-H.; Wurst, K.; Launay, J.-P. *Organometallics* **1997**, *16*, 392.
- Zhang, X.; Wang, J.; Gao, Y.; Zeng, X. C. *ACS Nano* **2009**, *3*, 537.
- Werner, H. One Deck More: The Chemical "Big Mac". In *Landmarks in Organo-Transition Metal Chemistry: A Personal View*; Springer: New York, 2009; p 177.
- Beck, V.; O'Hare, D. *J. Organomet. Chem.* **2004**, *689*, 3920.
- Kudinov, A. R.; Rybinskaya, M. I.; Struchkov, Yu.T.; Yanovskii, A. I.; Petrovskii, P. V. *J. Organomet. Chem.* **1987**, *336*, 187.
- Kudinov, A. R.; Filchickov, A. A.; Petrovskii, P. V.; Rybinskaya, M. I. *Russ. Chem. Bull.* **1999**, *48*, 1352.
- Herberich, G. E.; Englert, U.; Marken, F.; Hofmann, P. *Organometallics* **1993**, *12*, 4039.
- Lumme, P. O.; Turpeinen, U.; Kudinov, A. R.; Rybinskaya, M. I. *Acta Crystallogr.* **1990**, *C46*, 1414.
- Watson, E. J.; Virkaitis, K. L.; Li, H.; Nowak, A. J.; D'Acchioli, J. S.; Yu, K.; Carpenter, G. B.; Sweigart, D. A.; Chung, Y. K. *Chem. Commun.* **2001**, 457.
- Oh, M.; Reingold, J. A.; Carpenter, G. B.; Sweigart, D. A. *Coord. Chem. Rev.* **2004**, *248*, 561.
- Reingold, J. A.; Virkaitis, K. L.; Carpenter, G. B.; Sun, S.; Sweigart, D. A.; Czech, P. T.; Overly, K. R. *J. Am. Chem. Soc.* **2005**, *127*, 11146.
- Kudinov, A. R.; Rybinskaya, M. I. *Russ. Chem. Bull.* **1999**, *48*, 1615.
- Siebert, W.; Kudinov, A. R.; Zanello, P.; Antipin, M. Y.; Scherban, V. V.; Romanov, A. S.; Muratov, D. V.; Starikova, Z. A.; Corsini, M. *Organometallics* **2009**, *28*, 2707.
- Lauber, J. W.; Elian, M.; Summerville, R. H.; Hoffmann, R. J. *Am. Chem. Soc.* **1976**, *98*, 3219.
- Freyberg, D. P.; Robbins, J. L.; Raymond, K. N.; Smart, J. C. *J. Am. Chem. Soc.* **1979**, *101*, 892.
- Son, S. U.; Park, K. H.; Lee, S. J.; Chung, Y. K.; Sweigart, D. A. *Chem. Commun.* **2001**, 1290.
- Kim, J. E.; Son, S. U.; Lee, S. S.; Chung, Y. K. *Inorg. Chim. Acta* **1998**, *281*, 229.
- Herberich, G. E.; Jansen, U. *J. Organometallics* **1995**, *14*, 834.
- Werner, H.; Salzer, A. *Angew. Chem., Int. Ed. Engl.* **1972**, *11*, 930.
- Werner, H. *J. Organomet. Chem.* **1980**, *200*, 335.
- Biryukov, B. M.; Struchkov, Y. T. *Russ. Chem. Rev.* **1970**, *39*, 789.
- Cordero, B.; Gomez, V.; Platero-Prats, A. E.; Reves, M.; Echeverria, J.; Cremades, E.; Barragan, F.; Alvarez, S. *Dalton Trans.* **2008**, 2832.
- Barlow, S.; O'Hare, D. *Chem. Rev.* **1997**, *97*, 637.
- Merkert, J. W.; Davis, J. H., Jr.; Geiger, W. E.; Grimes, R. N. *J. Am. Chem. Soc.* **1992**, *114*, 9846.
- Schmitz, D.; Fleischhauer, J.; Meier, U.; Schleker, W.; Schmitt, G. *J. Organomet. Chem.* **1981**, *205*, 381.
- Struchkov, W. T.; Andrianov, V. G.; Salnikova, T. N.; Lyatfiov, I. R.; Materikova, R. B. *J. Organomet. Chem.* **1978**, *145*, 213.
- Kudinov, A. R.; Loginov, D. A.; Starikova, Z. A.; Petrovskii, P. V.; Corsini, M.; Zanello, P. *Eur. J. Inorg. Chem.* **2002**, 3018.
- Dubler, E.; Textor, M.; Oswald, H. R.; Jameson, G. B. *Acta Crystallogr. B* **1983**, *39*, 607.
- Schottenberger, H.; Wurst, K.; Griesser, U. J.; Jetli, R. K. R.; Laus, G.; Herber, R. H.; Nowik, I. *J. Am. Chem. Soc.* **2005**, *127*, 6795.
- Watson, E. J. Unpublished results. Seattle University, Seattle, 2013.
- Sarazin, Y.; Hughes, D. L.; Kaltsoyannis, N.; Wright, J. A.; Bochmann, M. *J. Am. Chem. Soc.* **2007**, *129*, 881.
- Trost, B. M.; Older, C. M. *Organometallics* **2002**, *21*, 2544.
- Steinmetz, B.; Schenk, W. A. *Organometallics* **1999**, *18*, 943.
- Sun, S.; Yeung, L. K.; Sweigart, D. A.; Lee, T.-Y.; Lee, S. S.; Chung, Y. K.; Switzer, S. R.; Pike, R. D. *Organometallics* **1995**, *14*, 2613.
- Sheldrick, G. M. *Bruker/Siemens Area Detector Absorption Correction Program*; Bruker AXS: Madison, WI, 1998.
- SHELXTL-6.10, *Program for Structure Solution, Refinement and Presentation*; Bruker AXS: Madison, WI, 2000.